PROCEEDINGS, 46th Workshop on Geothermal Reservoir Engineering
Stanford University, Stanford, California, February 15-17, 2021
SGP-TR-218

Nanobubbles as Corrosion and Scale Inhibitor

Masami Nakagawa[1], Arata Kioka[2], Asuki Aikawa[3], Ken Tagomori[2], Toru Kodama[2], and Satoshi Anzai[4]

[1]Department of Mining Engineering, 1500 Illinois St. Golden CO 80401 USA

[2]Gas Resources Department, Saibu Gas Co., Ltd., Fukuoka, Japan

[3]Department of Earth Resources Engineering, Kyushu University, Fukuoka, Japan

[4]Anzaikantetsu, Tsurumaki, Yokohama, Kanagawa, Japan

mnakagaw@mines.edu

Keywords: Scaling, Corrosion, Inhibitor, Nanobubbles

ABSTRACT

Geothermal resources with lower temperatures highlight many successful industrial applications; however, many share a common problem of scaling and/or corrosion. The cost to mitigate the problems with scaling and corrosion should not be underestimated so that the operators can better plan for the maintenance. It is also increasingly becoming difficult to justify using chemical agents to prevent these problems because of the elevated level of environmental concerns. The authors have started to investigate environmentally friendly and cost-effective ways to solve these problems. In this paper, we will share our preliminary experimental results on nanobubble usage as a corrosion and scale inhibitor.

1. INTRODUCTION

Nanobubbles are used for many engineering, environmental, biological and medical applications, and many beneficial results have been reported [Michailidi et al, 2019]. Although these benefits sometimes outweigh uncertain scientific reasoning why nanobubbles behave and provide benefits as they do, we need to make sure that basic scientific understanding is the driving force for a continued progress for the research. Particles and bubbles that are smaller than 1 micron are nanoparticles and nanobubbles. It is noted that handling a single nano-size material in either dry or wet environment is extremely difficult, and it pauses a great challenge with the characterization of a single entity. Nanopartilces and nanobubbles can be measured by similar methods such as Dynamic Light Scattering; however, particles are solid and bubbles are filled with gases. There is no mass transfer across the shell of a solid nanoparticle unless it is designed to function as such. On the contrary, gases in nanobubbles are concentrated and highly pressurized, and the gases are transferred to the surrounding liquid until the liquid is saturated by the gases to lose the concentration gradient or the internal pressure of nanobubbles is equilibrated against the fluid pressure. These gases are responsible for altering chemical environment of the surrounding fluid. Thus, the progress in understanding of the behavior of nanobubbles requires the understanding of physicochemical behavior of a single nanobubble and/or bulk of nanobubbles. This distinguishes the research approach to gain scientific understanding of nanobubble-behavior from that of nanoparticles. This is a demanding task for nanobubble researchers, and thus the progress has been somehat hindered. In this paper, we first briefly introduce our understanding of nanobubble behavior in geothermal settings and explain why nanobubbles should be considered as an alternative inhibitor against corrosion and/or scaling.

2. PHYSICOCHEMICAL PROPERTIES OF NANOBUBBLES

One of the most interesting size-dependent behavior of nanobubbles is due to their lack of buoyancy. Due to the small size, the buoyancy force on a single nanobubble, which is nothing but an unbalanced force on a single nanobubbles, is in the same order of the forces that are responsible for their Brownian motion. As such, nanobubbles wonder around in the water for an extended period of time [Ohgaki et al, 2010] instead of rising to the surface and vanish. The electrostatic interaction between nano-bubbles are also significant enough to discourage their coalescence leading to their stable existence as nano-bubbles, not as micro-bubbles [Ruckenstein 2013]. It has also been reported that the pH does not significantly influence the structural stability of nanobubbles. Surface nanobubbles have been recognized to make a strong impact on the solid-liquid interface as they change the two-phase contact to a three-phase contact. The wettability and slippage of a droplet containing nanobubbles on the solid surface [Li et al, 2016], for example, need to be understood better. In addition, surface nanobubbles are stable with respect to a temperature increase up to the boiling point of water because they can pin a microdroplet from the receding water over the surface[Zhang et al, 2014]. Finally, what is relevant to geothermal scaling is the fact that surface nanobubbles yield “superstability”; they are stable under large reduction of water pressure down to -6MPa [Boker et al, 2007]. Thus the use of nanobubbles holds promise in enabling to optimize the surface condition by controlling the nature of interface, allowing a broad range o geothermal applications. In addition, the use of nanobubbles will benefit from preventing chemical pollution and reducing cost for maintaining geothermal infrastructures, compared with the chemical products commonly used in geothermal industries.

2.1 Nanobubbles as an Inhibitor

2.1.1. Bubble mattress

Nanobubbles can strongly influence fluid flows along the microscopically rough but hydrophobic surfaces. Nanobubbles attached to the surface can have a lifetime of many hours, several days [Weijs and Lohse, 2013] and withstand near-boiling temperatures [Zhang et al., 2014]. In addition, nanobubbles can stay longer on a rough surface with the help of a "pinning" force on a rougher surface [Wang and Bhushan, 2010]. These recent experimental findings suggest that nanobubbles may be much more stable on the hydrophobic microscopically rough surface than the larger microbubbles. In conducting our field experiment, we assumed that nanobubbles generated in our experiments would be present on the immersed coupon surfaces at around 80°C for many hours.

Hydrodynamic boundary condition at solid walls is expressed by the Navier boundary condition. A slip length of a liquid at a solid interface is then expressed through $u = b(\partial u/\partial z)_0$, where u is the slip velocity at the solid wall, b is the slip length, and $(\partial u/\partial z)_0$ is the velocity gradient at the wall in the normal direction [Tabeling, 2005]. This indicates that a larger slip length means a lower drag of liquid flow at the interface. Surface nanobubbles on the solid interface thus increase the slip length, while the slippage is also influenced by surface roughness and wettability [Yen, 2015].

Once a few nanobubbles are present on the steel surface, the slip length may first decrease and the frictional force on the steel wall may decrease; however, the slip length will then increase with an increase of the surface coverage by nanobubbles [Maali and Bhushan, 2013; Wang and Bhushan, 2010; Hyväluoma et al., 2011; Li et al., 2016] and a decrease in the contact angle of nanobubbles on a rougher surface [Yen, 2015; Li et al., 2016] due to steel erosion/corrosion, leading to the reduction of the wall friction and enhance a wettability on the rough steel surface. After a continuous injection of nanobubbles, the slip length further increases when nanobubbles cover greater parts of the steel surface. We propose that the surface nanobubbles could act as a surface coating material for (1) inhibiting initiation of corrosion by increasing the slip length, and/or (2) preventing from exposing the initiated active interface to the acid geothermal fluid by acting as a bubble mattress (Figure 1a). These processes represent an important contribution of surface nanobubbles to the material coating at the acidic geothermal medium that may have a broader significance.

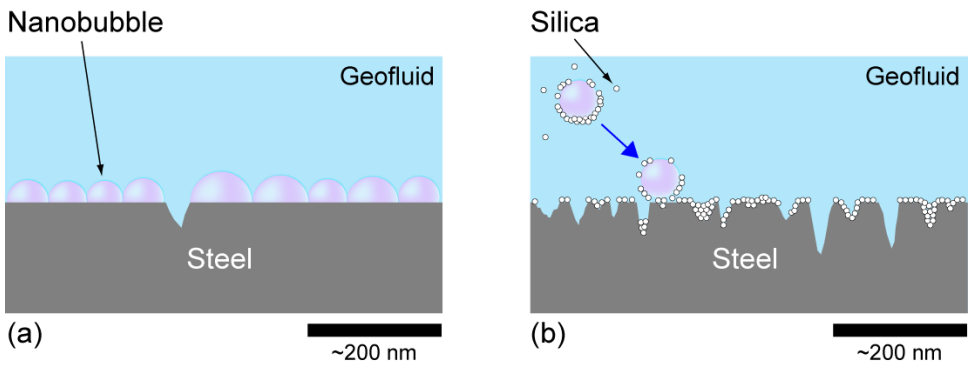

Figure 1: Schematic illustration of mechanism of inhibiting corrosion by nanobubbles. (a) Bubble mattress. (b) Silica precipitation.

2.1.2. Silica precipitation

We assume that silica precipitation contributes to inhibiting metallic corrosion in the acidic geothermal fluid. Precipitation of amorphous silica is common in high-enthalpy geothermal power plants, where fluids are rapidly cooled during geothermal energy production [van den Heuvel et al., 2018]. In geothermal environment, this silica scaling problem is of the same importance of metallic corrosion. On the other hand, Mundhenk *et al.* [2013] have suggested that scaling accompanies corrosion of mild steels at moderate temperatures in geothermal power plants. Moreover, several studies have also found that, once an initial layer of amorphous silica precipitates forms, it probably hampers the underlying steel surface from further reaction with geothermal fluid [Meier et al., 2014; van den Heuvel et al., 2016]. Therefore, silica precipitates may indeed act as inhibiting corrosion in an acidic moderate-temperature geothermal fluid.

Zeta-potential measurements of silica colloids as a function of pH show that the isoelectric point of silica nanoparticles is close to pH 2. In the pH of 2 to 6, the zeta potential of silica generally ranges from 0 to −30 mV, indicating the surface of amorphous silica is negatively charged and functionalized with Si-O^- groups [Bai et al., 2009]. In contrast, nanobubbles are generally positively charged in the solutions of pH < 4 [Takahashi, 2005; Calgaroto et al., 2014; Zhu et al., 2016]. Surface

nanobubbles can thus electrochemically adsorb nanoparticles [Zhou et al., 2019] in the studied acidic fluid (pH~3.5), resulting in promoting silica polymerisation and/or nucleation of silica monomers and their succeeding growth on the metallic surface. Therefore, nanobubbles can be an additive for generating a nano-silica blanket on the metallic surface to isolate the surface from flowing acidic geothermal water, when precipitated quantities of amorphous silica are moderate (Figure 1b).

2.1.3 Inhibition Effectiveness of Nanobubbles

The acceptable corrosion rate for materials is generally considered to be below 0.1 mm/year, given a certain corrosion allowance and a 20-year life. However, corrosion in an acidic geothermal fluid environment is much severe, ranging from a couple of millimetres per year in the moderate fluid environment to more than 100 mm/yr in the high-temperature and high-fluid velocity environment. The pH-adjustment is thus one of the most common methods for inhibiting such intensive corrosion, but it can also easily change the fluid chemistry which may produce undesired products. In contrast, we found that nanobubbles as a chemically benign, environmental-friendly, easy-to-use and low-cost additive agent had good corrosion inhibition effectiveness, probably by acting as bubble mattress and/or promoting slight precipitation of silica on the steel surface.

We now define the corrosion inhibition effectiveness of low-carbon steels by nanobubbles and relate to the effectiveness by pH-adjustment, by calculating and simulating long-term corrosion rates. First, the corrosion rates of immersed coupons can be approximated by the weight loss rate measured in the immersion corrosion test. The greater weight loss during the test represents the higher corrosion rate. Assuming uniform corrosive recession, the corrosion rate $C_r(t)$ (mm/year) of the coupon is obtained from:

$$C_r(t) = \frac{|\Delta m(t)|}{M} \times \delta \times \frac{24\times365}{t},$$

where $\Delta m(t)$ (g) is the weight loss, M (g) is the mass of given coupon before immersion test, and δ (mm) is the thickness of coupon (1 mm). The corrosion rate on a coupon $C_r(t)$ immersed in the reference fluid decreased gradually from 9.49 mm/yr to 5.28 mm/yr through time, while those immersed in the nanobubbles fluid ranged from 7.21 mm/yr to 3.39 mm/yr (Figure 2). Second, we used a corrosion model for mild steel in aqueous solutions developed by Nesic *et al.* [1966]. Here we simulated a time-variable corrosion rate of low-carbon steel for tested 7 days using the software made by Nešić *et al.* [2009]. Because flow properties in immersion experiments were uncertain, we used the corrosion rates of the coupons immersed in the reference fluid, an average temperature (80°C) and an average pH value (3.5) and chemical compositions of studied geothermal fluid (Table 1), to inversely determine the optimum values of flow properties that best fit the corrosion rates of the coupons immersed in the reference fluid. Third, we changed pH values to find the optimum pH value that best fits the corrosion rates of the coupons immersed in the nanobubbles fluid, while other chemical parameters and flow parameters were unchanged. From this calculation, we found the equivalent pH for the corrosion rates of the coupons immersed in the nanobubbles fluid was 3.7 (Figure 2), indicating that our air-nanobubble treatment in the acidic geothermal fluid was comparable to neutralising 0.2 in pH by pH-adjustment.

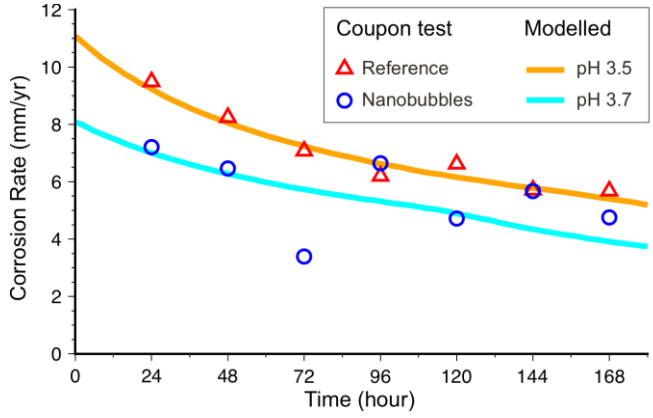

Figure 2: Corrosion rates of the coupons immersed in the reference fluid (red triangles) and the nanobubbles fluid (blue circles) with modelled corrosion rates at pH of 3.5 (orange line) and 3.7 (cyan line).

Table 1: Chemical composition of studied geothermal fluid (mg/L).

Na	K	Ca	Mg	Cl	SO_4	HCO_3	Fe	F	SiO_2
1090	198	8.0	360	1640	489	< 1	4027	4.3	855

3. FIELD EXPERIMENT: CORROSION TESTS

In 2018, we started to conduct a series of immersion corrosion tests at the Hatchobaru Geothermal Power Plant (Kyushu Electric Power Co., Inc.) in Oita Prefecture, Japan. The experimental set up and the chemical composition of their geothermal water are shown in Figure 3 and Table 1, respectively. We diverted acidic geothermal water from the separator of the power plant. The test coupons for corrosion experiments were immersed in the geothermal water overflowed continuously in two heat-resisting polypropylene containers (700 × 330 × 350 mm) (Figure 3b). The geothermal fluid in the containers was constantly stirred by small water pumps. Two different fluid environments were created: untreated geothermal fluid (Reference fluid) and geothermal fluid mixed with air-nanobubbles. In this study, we continuously generated air-nanobubbles and injected into the geothermal fluid for up to 7 days. Nanobubbles were produced using a patented ultrafine pore ceramic-nozzle generator (Anzaikantetsu Co., Ltd., Yokohama, Japan) at 0.2 MPa controlled by an air compressor. This nanobubble generator was expected to produce 3×10^9 bubbles per millilitre with a mean diameter of 85 nm. The temperature and pH of the geothermal fluid in the containers were within 75–85°C and 3.4–3.6, respectively. The flow rate into and out of the containers varied between 0.5 and 2.0 L/min because we could not control the flow rates of geothermal fluid leaving the separator.

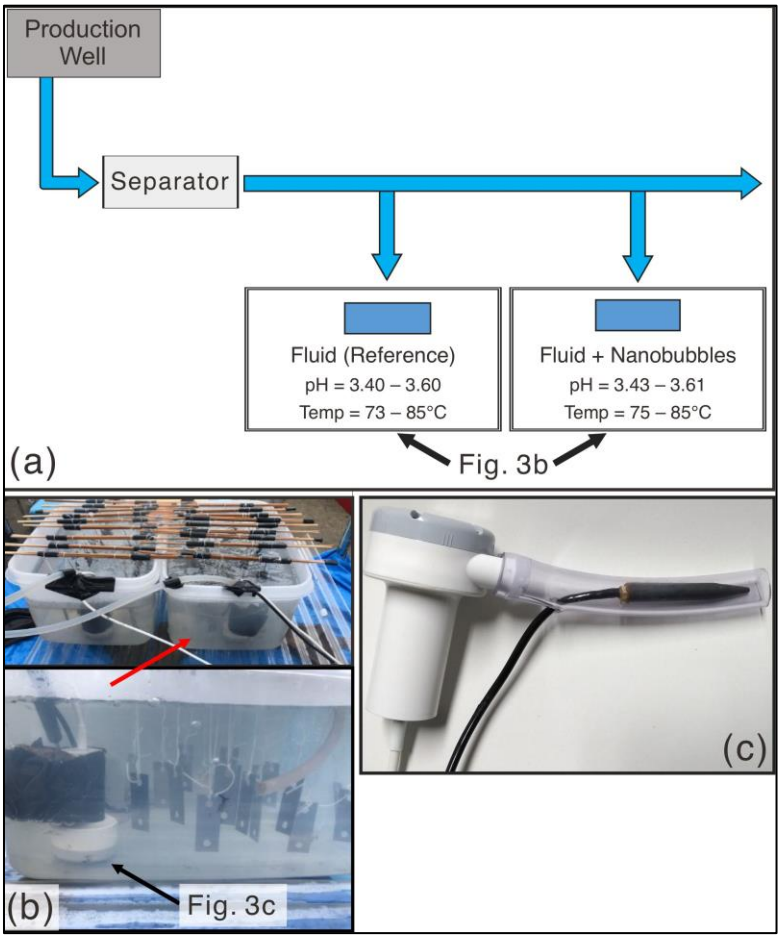

Figure 3: (a) Schematic illustration of immersion corrosion experiments. (b) Photos of immersion corrosion experiments. (c) Ceramic nozzle type nanobubble generator used in this study.

We used a low-carbon steel "Steel Plate Cold Commercial (SPCC)" (JIS G3141 Standards) whose chemical composition is the following in wt% : C ≤ 0.15, Mn ≤ 0.10, P ≤ 0.10, S ≤ 0.035, and few negligible impurities. A SPCC coupon (50 × 20 × 1 mm) for corrosion tests was made with two 6.5-mm diameter holes. All the new coupons were weighed between 8,655 and 8,705 mg. Each immersed coupon was systematically taken out of the reference fluid and the air-nanobubbles fluid after 24, 48, 72, 96, 120, 144, and 168 hours. The tested coupons were rinsed carefully by distilled water, dried, and weighed again to calculate the loss of its mass. To evaluate inhibition efficiency of the nanobubble fluid, we calculated the "corrosion inhibition effectiveness" $\eta(t)$(%) of the coupons immersed in the air-nanobubbles fluid for t (hr):

$$\eta(t) = \left(\Delta m_{ref}(t) - \Delta m_{nb}(t)\right)/\Delta m_{ref}(t) \times 100,$$

where $\Delta m_{ref}(t)$ (g) and $\Delta m_{nb}(t)$ (g) are the weight losses of the coupons immersed in the reference fluid and the air-nanobubbles fluid for t (hr), respectively. Here, when the weight loss of the coupon is less, it is the indication of better protection against corrosion. In the laboratory, we analyzed surface microstructure of weighed coupons by Scanning Electron Microscope (SEM) using a HITACHI SU3500 at Center of Advanced Instrumental Analysis, Kyushu University. We also determined the chemical composition of corrosion on the coupon surface by Energy-dispersive X-ray spectroscopy (EDX).

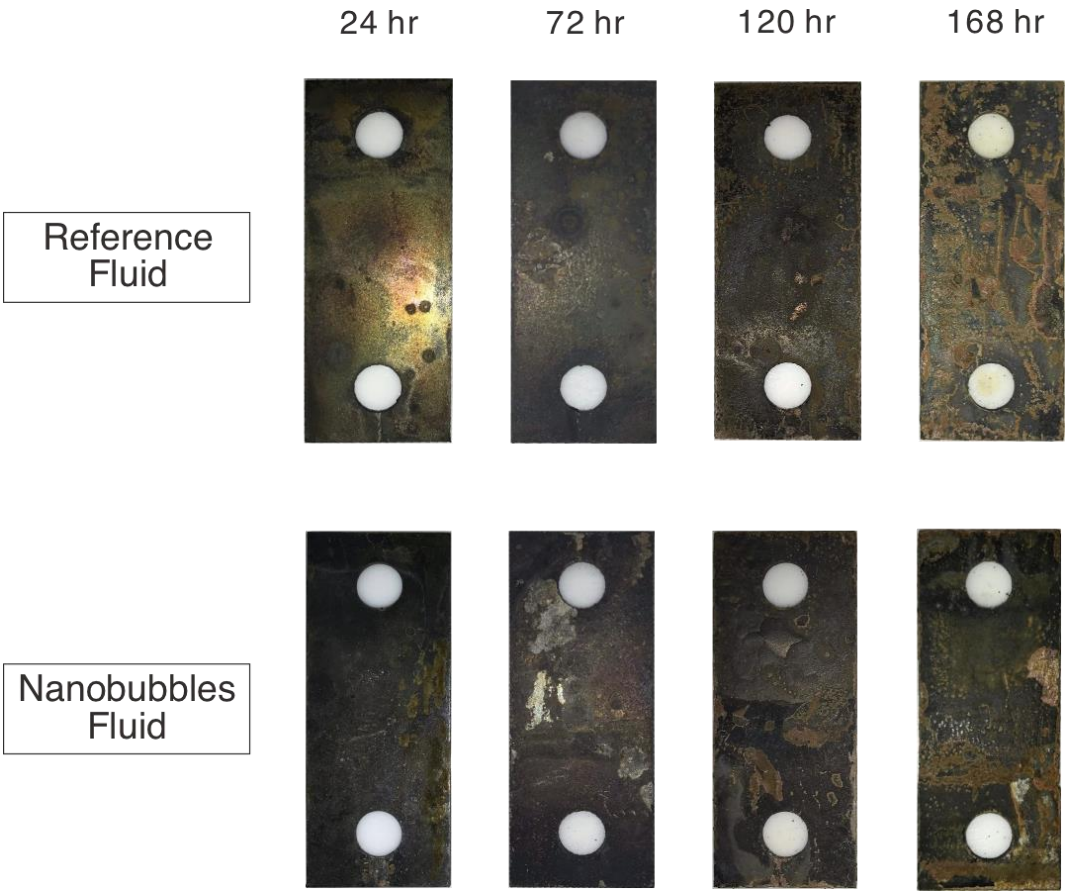

Figure 4: Photos of the coupons from the reference fluid and air-nanobubble fluid after 24 hr, 72 hr, 120 hr, and 168 hr of immersion test.

Even after 24 hours of immersion testing, both the coupons from the reference fluid and air-nanobubble fluid already lost much of their metallic lustre (Figure 4). Corrosion damage was then more significant in the coupons that were immersed for a longer time. Corrosion damage with abrasion was apparent in the coupons after 72 and 120 hours of immersion test. Blisters with a width of up to 6 mm were also present on the surface of immersed coupons, and they are probably cathodic blisters caused by the hydrogen gas formation given their size. The coupons after 168 hr of immersion further experienced extensive corrosion with most their colour turning reddish-brown.

Weight losses of the coupons immersed in the reference fluid increased gradually with time, ranging from 226 mg (2.6% of the original mass before immersion test) to 946 mg (10.9%). The rate of weight loss with the reference fluid was highest for the coupon immersed for 24 hr (226 mg/day) and the average rate of weight loss 166 mg/day. Similarly, weight losses of the coupons immersed in the air-nanobubbles fluid also generally increased through time, ranging from 171 mg (2.0% of the original mass before immersion test) to 810 mg (9.1%) with the average weight loss rate of 132 mg/day, while the changes were rather fluctuating than those in the reference fluid. The fluctuation might be due to an unsteady fluid flow rate to the tested container and/or an unsteady rate of nanobubble generation. Notably, weight losses of the coupons immersed in the air-nanobubbles fluid after 24, 48, 72, 120, and 168 hours of immersion were significantly smaller than those in the reference fluid after the respective time of immersion (Figure 5). The corrosion inhibition effectiveness (η) of the coupons immersed for 24, 48, 72, 120, and 168 hours was 24%, 21%, 52%, 28%, and 16%, respectively.

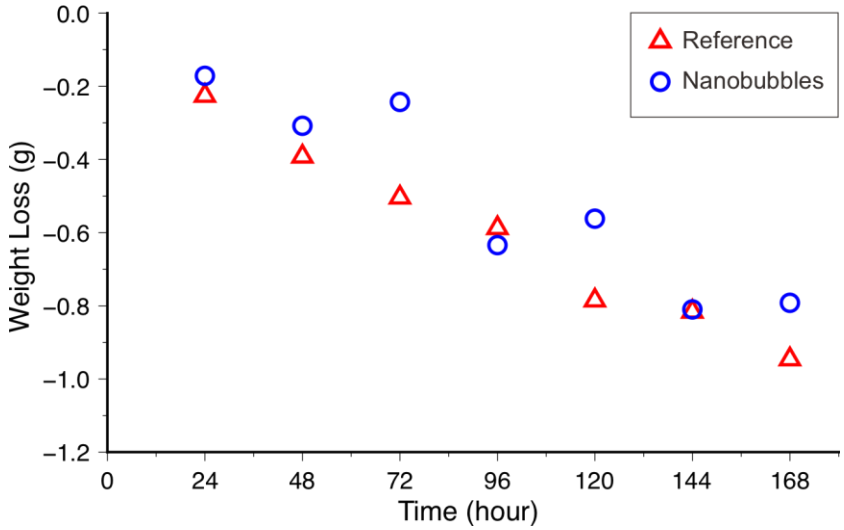

Figure 5: Weight losses of the coupons immersed in the reference fluid (red triangles) and air-nanobubble fluid (blue circles).

Microstructure analyses using SEM revealed the progress of corrosion on the coupons (Figure 6). Microstructure analyses showed that the abrasion on the coupon surface was already apparent in 24 hours of immersion testing both in the reference fluid and air-nanobubble fluid (Figure 6b). It is interesting to note that when compared with the coupons after 72, 120, and 168 hours of immersion in the reference fluid, the coupons immersed in the air-nanobubbles fluid for the respective time had less abrasion (Figures 6c–6e).

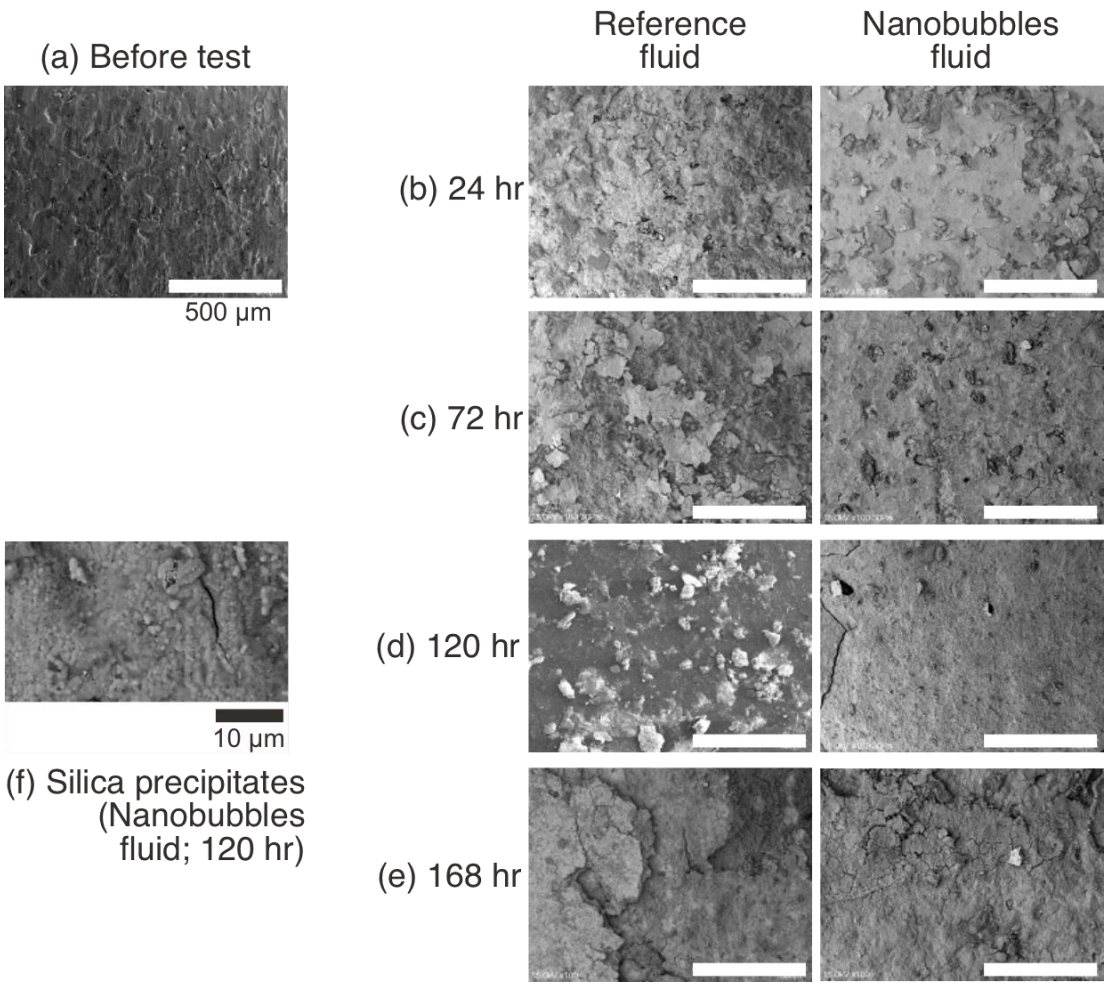

Figure 6: Representative SEM images of the coupons from the reference fluid and air-nanobubble fluid (a) before immersion corrosion testing, (b) after 24 hr of immersion, (c) after 72 hr of immersion, (d) after 120 hr of immersion, and (e) after 168 hr of immersion. A white scale bar indicates 500 µm. (f) Close-up SEM image of the coupon immersed in the air-nanobubble fluid for 120 hr, showing nanoscopic silica precipitates. A black scale bar indicates 10 µm.

Microanalyses using EDX identified changes in chemical composition on the coupon surface with immersion time (Figure 7). In general, Fe of the coupon surfaces decreased with immersion time, while Fe of the coupon immersed in the nanobubbles fluid is lower than that of the coupon immersed in the reference fluid. This relates to that surface concentration of iron oxides in the coupons immersed in the nanobubbles fluid is lower than that in the reference fluid for 48, 72, 96, 120, and 144 hours of immersion testing. The EDX results also revealed that Si concentrations of the coupons immersed for 48–168 hours in the nanobubbles fluid were higher than those in the reference fluid, as suggested by SEM images (Figure 6f). Si concentrations immersed in both the reference fluid and nanobubbles fluid for the first 24 hours were equally quite low.

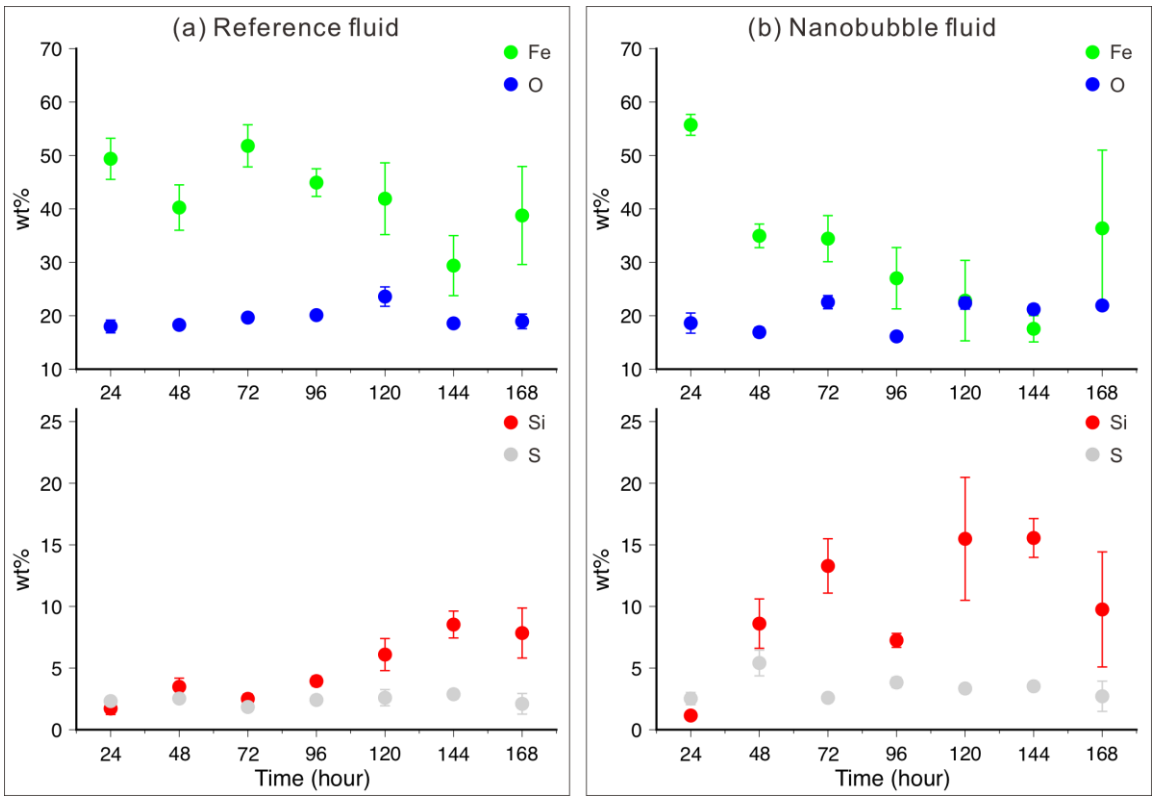

Figure 7: Chemical composition on the surfaces of immersed coupons (wt%) analysed by EDX. (a) Coupons immersed in reference fluid and (b) coupons immersed in air-nanobubble fluid. The concentrations Fe, O, Si and S of the coupons before the immersion test analysed by EDX were 92.7±0.8, 1.73±0.07, 0.0, 0.12±0.04 wt%, respectively.

4. CONCLUDING REMARK

We have examined, for the first time to our knowledge, the ability of nanobubbles against corrosion on test coupons immersed in an acidic geothermal fluid. Results of our immersion corrosion experiments revealed that the weight loss of coupons immersed in the fluid with air-nanobubbles was reduced as much as 50% of the weight of the coupons in the untreated reference fluid. In addition, microstructure analyses showed retarded abrasion from the surface of the coupons immersed in the nanobubbles fluid. Chemical composition analyses suggested lower concentrations of iron oxides and higher concentrations of silica in the coupons immersed in the nanobubbles fluid. This should be related to the unique nature of nanobubbles that leads to influence liquid-steel interface. As a cautionary remark, we note that the interpretation of how nanobubbles attribute to these corrosion behaviours may not be unique, because of the intrinsic complexities of corrosion and nanobubbles. Below, we discuss two aspects of our findings, and they are (1) possible mechanisms with respect to how nanobubbles inhibit corrosion of low-carbon steels and (2) how much corrosion inhibition effectiveness of low-carbon steels by nanobubbles is equivalent to that by adjusting pH.

Acknowledgment

The authors are grateful to A. Ueda, T. Yokoyama, K. Yonezu, and Y. Kiyota for their fruitful discussions and suggestions throughout the work presented in the manuscript. This work was partly supported by the project “Research and development of geothermal power generation technology — Development of technology for advanced use of geothermal energy — Development of chemical processing systems to properly utilize and brine” from the New Energy and Industrial Technology Development Organization (NEDO), Japan.

REFERENCES

Bai, S., Urabe, S., Okaue, Y., and Yokoyama, T.: Acceleration effect of sulfate ion on the dissolution of amorphous silica. J. Colloid Interf. Sci., **331**, (2009), 551–554. https://doi.org/10.1016/j.jcis.2008.11.076

Borkent BM, Dammer SM, Schönherr H, Julius Vancso G, and Lohse D.: Superstability of Surface Nanobubbles, *Phys Rev Lett*, **98**, (2007), 204502.

Calgaroto, S., Wilberg, K.Q., and Rubio, J.: On the nanobubbles interfacial properties and future applications in flotation, *Miner. Eng*., **60**, 33–40. http://dx.doi.org/10.1016/j.mineng.2014.02.002

Hyväluoma, J., Kunert, C., and Harting, J.: Simulations of slip flow on nanobubble-laden surfaces, *J. Phys. Condens. Matter*, **23**, (2011), 184106. https://doi.org/10.1088/0953-8984/23/18/184106

Li D, Jing D, Pan Y, Bhushan B, and Zhao X.: Study of the Relationship between Boundary Slip and Nanobubbles on a Smooth Hydrophobic Surface, *Langmuir*,**32**, (2016), 11287–11294. https://doi.org/10.1021/acs.langmuir.6b02877

Meier, D., Gunnlaugsson, E., Gunnarsson, I., Jamtveit, B., Peacock, C., and Benning, L.: Microstructural and chemical variation in silica-rich precipitates at the Hellishei geothermal power plant. *Mineral. Mag.* ,**78(6),** (2014),1381–1389. https://doi.org/10.1180/minmag.2014.078.6.04

Michailidi, E., Bomis, G., Varoutoglou, A., Efthimiadou, E., Mitropoulos, A., and Favvas, E. P.: Fundamenals and applications of nanobubbles, *Interface Science and Technoloy*, **30**, (2019), 69-99.

Mundhenk, N., Huttenloch, P., Sanjuan, B., Kohl, T., Steger, and H., Rorn, R.: Corrosion and scaling as interrelated phenomena in an operating geothermal power plant. *Corros. Sci.*, **70**, (2013), 17–28. https://doi.org/10.1016/j.corsci.2013.01.003

Nesic, S., Postlethwaite, J., and Olsen, S.: An Electrochemical Model for Prediction of Corrosion of Mild Steel in Aqueous Carbon Dioxide Solutions. Corrosion **52(4)**, (1996), 280−294. https://doi.org/10.5006/1.3293640

Nešić, S., Li, H., Huang, J., and Sormaz, D.: An Open Source Mechanistic Model for CO2/H2S Corrosion of Carbon Steel. NACE International Corrosion/09, Houston, TX, paper no. 09572, (2009).

Ohgaki K, Khanh NQ, Joden Y, Tsuji A, and Nakagawa T.: Physicochemical approach to nanobubble solutions. *Chem Eng Sci* , **65**, (2010),1296–1300. https://doi.org/10.1016/j.ces.2009.10.003

Ruckenstein E.: Nanodispersions of bubbles and oil drops in water, *Colloids Surf A Physicochem Eng Asp*, **423**, (2013),112–114.

Tabeling, P.: Introduction to Microfluidics, *Oxford University Press, UK*, (2005), 310 p.

Takahashi, M.: ζ Potential of Microbubbles in Aqueous Solutions: Electrical Properties of the Gas-Water Interface. *J. Phys. Chem. B*, **109**, (2005). 21858−21864. https://doi.org/10.1021/jp0445270

van den Heuvel, D.B., Gunnlaugsson, E., and Benning, L.G.: Passivation of metal surfaces against corrosion by silica scaling, *Proceedings of the 41st Workshop on Geothermal Reservoir Engineering*, SGP-TR-209, 2016.

Wang, Y. and Bhushan, B.: Boundary slip and nanobubbles study in micro/nanofluidics using atomic force microscopy, Soft Matter, **6**, (2010), 29−66. https://doi.org/10.1039/B917017K

Weijs, J.H. and Lohse, D,: Why Surface Nanobubbles Live for Hours, *Phys. Rev. Lett.*, **110**, (2013), 054501. https://doi.org/10.1103/PhysRevLett.110.054501

Yen, T.-H.: Effects of wettability and interfacial nanobubbles on flow through structured nanochannels: an investigation of molecular dynamics, *Mol. Phys.*, **113**, (2015), 3783–3795. https://doi.org/10.1080/00268976.2015.1062928

Zhang X, Lhuissier H, Sun C, and Lohse D.: Surface Nanobubbles Nucleate Microdroplets, *Phys Rev Lett*, **112**, (2014), 144503. https://doi.org/10.1103/PhysRevLett.112.144503

Zhou, W., Niu, J., Xiao, W., and Ou, L.: Adsorption of bulk nanobubbles on the chemically surface modified muscovite minerals. Ultrason. Sonochem. **51**, (2019), 31−39. https://doi.org/10.1016/j.ultsonch.2018.10.021